Mitochondrial reactive oxygen species promote production of proinflammatory cytokines and are elevated in TNFR1-associated periodic syndrome (TRAPS)

Ariel C. Bulua,[1,4] Anna Simon,[2] Ravikanth Maddipati,[1] Martin Pelletier,[1] Heiyoung Park,[1] Kye-Young Kim,[3] Michael N. Sack,[3] Daniel L. Kastner,[2] and Richard M. Siegel[1]

[1]Immunoregulation Section, Autoimmunity Branch, and [2]Inflammatory Biology Section, Laboratory of Clinical Investigation, National Institute of Arthritis and Musculoskeletal and Skin Diseases, and [3]Laboratory of Mitochondrial Biology in Cardiometabolic Syndromes, Translational Medicine Branch, National Heart, Lung, and Blood Institute, National Institutes of Health, Bethesda, MD 20892
[4]Immunology Institute, Mount Sinai School of Medicine, New York, NY 10029

Reactive oxygen species (ROS) have an established role in inflammation and host defense, as they kill intracellular bacteria and have been shown to activate the NLRP3 inflammasome. Here, we find that ROS generated by mitochondrial respiration are important for normal lipopolysaccharide (LPS)–driven production of several proinflammatory cytokines and for the enhanced responsiveness to LPS seen in cells from patients with tumor necrosis factor receptor–associated periodic syndrome (TRAPS), an autoinflammatory disorder caused by missense mutations in the type 1 TNF receptor (TNFR1). We find elevated baseline ROS in both mouse embryonic fibroblasts and human immune cells harboring TRAPS-associated TNFR1 mutations. A variety of antioxidants dampen LPS-induced MAPK phosphorylation and inflammatory cytokine production. However, gp91^{phox} and p22^{phox} reduced nicotinamide adenine dinucleotide phosphate (NADPH) oxidase subunits are dispensable for inflammatory cytokine production, indicating that NADPH oxidases are not the source of proinflammatory ROS. TNFR1 mutant cells exhibit altered mitochondrial function with enhanced oxidative capacity and mitochondrial ROS generation, and pharmacological blockade of mitochondrial ROS efficiently reduces inflammatory cytokine production after LPS stimulation in cells from TRAPS patients and healthy controls. These findings suggest that mitochondrial ROS may be a novel therapeutic target for TRAPS and other inflammatory diseases.

CORRESPONDENCE
Richard M. Siegel:
rsiegel@nih.gov

Abbreviations used: CAPS, cryopyrin-associated periodic syndromes; CGD, chronic granulomatous disease; DHR, dihydrorhodamine 123; DPI, diphenylene iodonium; dTPP, decyl-TPP bromide; FAD, flavin adenine dinucleotide; MAPK, mitogen-activated protein kinase; MEF, mouse embryonic fibroblast; MitoQ, mitoquinone; NAC, N-acetyl-cysteine; NADPH, reduced nicotinamide adenine dinucleotide phosphate; NOX, NADPH oxidase; phox, phagocyte oxidase; qRT-PCR, quantitative RT-PCR; ROS, reactive oxygen species; TNFR1, tumor necrosis factor receptor 1; TRAPS, TNFR1-associated periodic syndrome

Reactive oxygen species (ROS) have been implicated in inflammatory diseases including rheumatoid arthritis (Filippin et al., 2008), multiple sclerosis (Gilgun-Sherki et al., 2004), thyroiditis (Burek and Rose, 2008), and type 1 diabetes (Chen et al., 2008). It has long been known that ROS perform essential roles in immune responses to pathogens, including bacterial killing through the production of superoxide by reduced nicotinamide adenine dinucleotide phosphate (NADPH) oxidases during the respiratory burst in activated macrophages and neutrophils (Lambeth, 2004; Kanayama and Miyamoto, 2007). NADPH oxidase (NOX)–derived ROS are critical in host defense, as patients with chronic granulomatous disease (CGD) or mice engineered to lack components of the NOXs have increased susceptibility to infection (Morgenstern et al., 1997; Shiloh et al., 1999).

Other work has elucidated a role for ROS in modulating immune responses through effects on signal transduction cascades, although the biochemical mechanisms by which ROS modify

A. Simon's present address is Dept. of General Internal Medicine, Radboud University, Nijmegen Medical Centre, Nijmegen, Netherlands.

This article is distributed under the terms of an Attribution–Noncommercial–Share Alike–No Mirror Sites license for the first six months after the publication date (see http://www.rupress.org/terms). After six months it is available under a Creative Commons License (Attribution–Noncommercial–Share Alike 3.0 Unported license, as described at http://creativecommons.org/licenses/by-nc-sa/3.0/).

The Rockefeller University Press $30.00
J. Exp. Med. Vol. 208 No. 3 519-533
www.jem.org/cgi/doi/10.1084/jem.20102049

The Journal of Experimental Medicine

these pathways are not always clear (Nathan, 2003). ROS have been implicated in the activation of signaling pathways such as mitogen-activated protein kinases (MAPK), NF-κB, and guanylate cyclase (Schmidt, 1992; Takada et al., 2003; Kamata et al., 2005), and have been shown to modulate B cell receptor signaling (Capasso et al., 2010), mast cell activation (Tagen et al., 2009), and cell adhesion (Sellak et al., 1994). TNF-induced mitochondrial ROS have been implicated in cell death through inhibition of MAPK phosphatases (Kamata et al., 2005). ROS have many sources, including peroxisomes, ubiquinone, cytosolic enzymes including cyclooxygenase, uncoupled nitric oxide synthases, and ERO1 in the endoplasmic reticulum (Landmesser et al., 2003; Sevier and Kaiser, 2008). It is believed, however, that in cells undergoing aerobic metabolism, the majority of ROS are produced as a byproduct of the mitochondrial electron transport chain (Chance et al., 1979; Balaban et al., 2005).

Recently, a role for ROS has emerged in the activation of the NLRP3 inflammasome, one pathway for generation of active caspase-1 and secretion of mature IL-1β (Zhou et al., 2010a). The NOX enzymes have been implicated as the source of ROS in inflammasome activation, as antioxidants thought to block NOXs and knockdown of p22 phagocyte oxidase (phox), a common subunit of four NOXs, resulted in diminished NLRP3 activation upon stimulation (Cruz et al., 2007; Pétrilli et al., 2007; Dostert et al., 2008). More recent work shows a role for mitochondrial damage in NLRP3 inflammasome activation (Zhou et al., 2010b). However, whether ROS directly activate the inflammasome has been called into question by data showing a distinct role for ROS in up-regulation of mRNA for inflammatory cytokines such as IL-1β and TNF(van de Veerdonk et al., 2010).

Tumor necrosis factor (TNF) receptor-associated periodic syndrome (TRAPS) is an autosomal dominant autoinflammatory disease associated with enhanced innate immune responsiveness. TRAPS is characterized clinically by recurrent fevers, abdominal pain (peritonitis), migratory rash, myalgia, and arthralgia. As with other autoinflammatory diseases, TRAPS can be complicated by the development of systemic amyloidosis caused by chronic inflammation and production of serum amyloid A (Hull et al., 2002). TRAPS is caused by mutations in the extracellular domain of the gene encoding TNF receptor 1 (TNFR1, TNFRSF1A, CD120a, and p55-TNFR), and >50 individual mutations have been identified to date (Touitou et al., 2004). TNFR1 is a prototypic member of the TNF superfamily, capable of inducing inflammation and cell death. TNFR1 molecules harboring TRAPS-associated mutations fail to interact with WT TNFR1 receptors or TNF and traffic abnormally in the cell, with retention and accumulation in the endoplasmic reticulum (Todd et al., 2004; Lobito et al., 2006; Simon et al., 2010). These mutations are referred to as structural mutations and are not found in the general population. Rare polymorphisms in TNFR1, such as those encoding R92Q and P46L mutations, are present in up to 5% of the healthy population and can also be associated with a TRAPS-like phenotype; these patients have milder inflammatory symptoms and rare development of amyloidosis (Ravet et al., 2006). TNFR1 with these polymorphisms behave like WT receptors in terms of receptor trafficking and TNF binding (Lobito et al., 2006).

Other autoinflammatory diseases, such as those associated with mutations in NLRP3/cryopyrin or IL-1β receptor antagonist, are specifically associated with IL-1β overproduction or excessive IL-1β signaling, and IL-1β blockade in these fever syndromes results in normalization of inflammatory parameters and robust clinical responses (Hoffman et al., 2004; Goldbach-Mansky et al., 2006). In TRAPS, however, heterozygous TNFR1 mutant cells produce higher levels of a wide variety of inflammatory cytokines, including IL-1β, TNF, and IL-6, in response to LPS stimulation as compared with WT cells, whereas TNFR1 homozygosity resembles TNFR1 deficiency (Simon et al., 2010). Pharmacological blockade of IL-1β or TNF has only partial effects on TRAPS symptoms, with some patients progressing to amyloidosis even on these therapies (Hull et al., 2002).

We have shown that one way in which mutant TNFR1 predisposes to enhanced inflammation in TRAPS is through increased activation of MAPKs, independent of TNF. Cells harboring TRAPS-associated TNFR1 mutations display spontaneous MAPK activation, as well as enhanced and prolonged MAPK activation after LPS stimulation (Simon et al., 2010). ROS can potentiate MAPK activation by inactivation of MAPK phosphatases through oxidation of their catalytic cysteine residues (Meng et al., 2002; Reth, 2002; Kamata et al., 2005). This leads to a sustained MAPK response that temporally resembles the MAPK response seen in TRAPS. For this reason, we have investigated the role that ROS play in abnormal signaling and inflammatory cytokine production in cells harboring TNFR1 mutations. ROS have been shown to contribute to normal inflammatory responses and to the pathophysiology of other autoinflammatory diseases. Recent work has demonstrated elevated baseline levels of ROS in the autoinflammatory cryopyrin-associated periodic syndromes (CAPS; Tassi et al., 2010). It was shown that IL-1β production could be blocked using the antioxidant drug diphenylene iodonium (DPI) in both CAPS patients and healthy donors. However, recent work using NOX2-deficient CGD patient cells found no defect in IL-1β secretion (van de Veerdonk et al., 2010), contradicting the notion that DPI inhibits IL-1β production through blockade of NOX-generated ROS. DPI has been shown, instead, to have an effect on transcription of inflammatory cytokine mRNA (van de Veerdonk et al., 2010). Thus, the mechanism of action of DPI may extend beyond NOXs.

To investigate the role of ROS in inflammatory signaling and the source of ROS generation, we studied ROS levels in TRAPS patient cells and mouse embryonic fibroblasts (MEFs) derived from a mouse model in which heterozygous TNFR1 mutations associated with TRAPS have been engineered into the mouse genome. We used antioxidants, genetic models, and metabolic measurements to exclude NOXs and identify the mitochondrial electron transport chain as the predominant

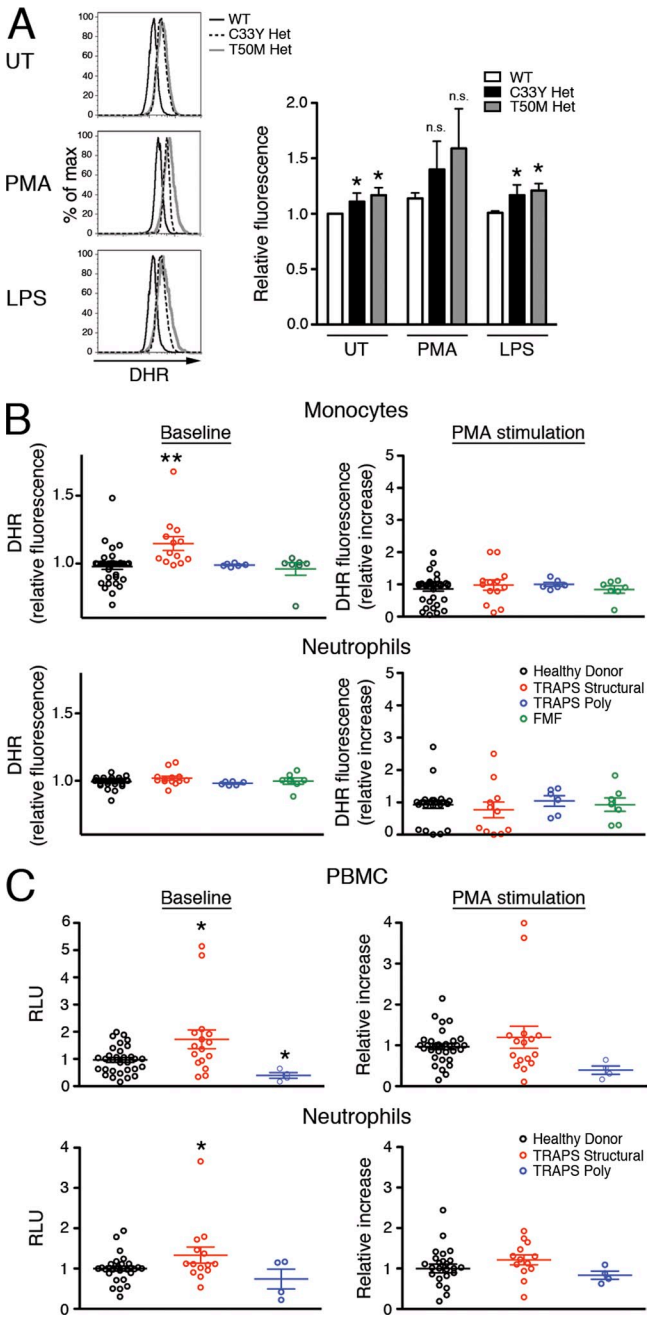

Figure 1. Increased ROS in TNFR1 mutant cells and peripheral blood cells from TRAPS patients. (A) WT, C33Y TNFR1 heterozygous, and T50M TNFR1 heterozygous MEFs were left untreated (UT) or were treated with PMA or LPS for 1 h. Cells were incubated with DHR and ROS levels were determined by flow cytometry. Bar graph shows results of four independent experiments and histograms show one representative experiment. n.s., not significant. Error bars represent the mean ± SEM. (B) Monocytes and neutrophils from healthy donors (n = 27–31), TRAPS patients with structural mutations (TRAPS structural; n = 11–13), TRAPS patients with R92Q polymorphisms (TRAPS poly; n = 6), or patients with familial Mediterranean fever (FMF; n = 7) were treated for 1 h with or without PMA. Cells were incubated with DHR, and ROS levels were determined by flow cytometry. Data are from 10 experiments; each symbol represents a unique patient. (C) PBMCs and neutrophils from healthy donors (n = 25–33), TRAPS patients with structural mutation (TRAPS structural; n = 13–16) and TRAPS patients with R92Q or P46L polymorphisms (TRAPS poly; n = 4) were analyzed for superoxide production with a kinetic chemiluminescent assay in the presence or absence of PMA. Data are from 11 experiments; each symbol represents a unique patient. RLU, relative luminescence units. Data were normalized to the mean WT or healthy donor result for each experiment. *, $P \leq 0.05$; **, $P < 0.01$.

source of ROS responsible for physiological inflammatory cytokine production in normal cells, as well as the hyperproduction of cytokines in cells from TRAPS patients and TRAPS model mice.

RESULTS

ROS are increased in cells harboring TRAPS-associated TNFR1 mutations

We have previously observed that MAPK activation is increased in cells harboring TRAPS-associated TNFR1 mutations and that exaggerated inflammatory responses in TRAPS depend on p38 and JNK MAPK (Simon et al., 2010). Because ROS are known to inactivate MAPK phosphatases and perpetuate MAPK activation (Kamata et al., 2005), we hypothesized that increased ROS may underlie the exaggerated MAPK signaling and inflammatory responses in TRAPS. We therefore investigated the baseline and induced levels of ROS in cells harboring TRAPS-associated TNFR1 mutations with the redox-sensitive probe dihydrorhodamine 123 (DHR). DHR, which rapidly diffuses through the cell membrane and is oxidized into the fluorescent compound rhodamine by free radicals, measures the total oxidative capacity of a cell. In T50M and C33Y TNFR1 heterozygous MEFs, we found that baseline ROS levels were elevated. The increase was small, but consistent and statistically significant. As expected, phorbol-12-myristate-13-acetate (PMA), which induces cells to undergo the NOX–dependent respiratory burst, further increased the ROS levels in both normal and mutant cells, but not out of proportion to the baseline levels. In contrast, LPS stimulation did not induce further ROS production in either normal or mutant cells (Fig. 1 A).

To determine whether elevated ROS could be detected in TRAPS patient cells, we examined ROS levels using the DHR assay in monocytes and neutrophils isolated from TRAPS patients with either structural TNFR1 mutations or TNFR1 polymorphisms, healthy control donors, or patients with the autoinflammatory disease familial Mediterranean fever. We found significantly elevated ROS levels at baseline in monocytes from TRAPS patients with structural TNFR1 mutations compared with monocytes from the other three groups (Fig. 1 B). After induction of the respiratory burst with PMA, the increase in ROS over baseline was not significantly different between monocytes from TRAPS patients and healthy controls. Similar to the MEFs, neither TRAPS patient nor control cells responded to LPS with an increase in ROS production (Fig. S1 A). We also examined neutrophils, which produce large amounts of ROS during the respiratory

burst (Nathan, 2006). We could not detect elevated baseline or induced ROS in neutrophils from TRAPS patients using this assay. We found no correlation between elevated ROS in TRAPS patient cells and C-reactive protein, specific TNFR1 mutation, flare status, or medications, suggesting that increased ROS production is an intrinsic feature of TRAPS rather than a result of symptoms or treatment at the time of sample collection (Fig. S1 B). We also measured ROS production with a luminol-based method that is very sensitive for superoxide production, and found higher baseline ROS levels in PBMCs from TRAPS patients with structural TNFR1 mutations, but similar induction of the respiratory burst with PMA (Fig. 1 C). In addition, the increased sensitivity of the luminol-based assay allowed detection of a slight elevation in neutrophil ROS levels in TRAPS cells that was not evident using the DHR assay. Although PBMCs from patients with TNFR1 polymorphisms appeared to generate less ROS using luminol detection, this is not likely to have functional consequences, as it has been previously shown that PBMCs from patients with TNFR1 polymorphisms respond normally to LPS (Simon et al., 2010). Collectively, these data indicate a baseline elevation in ROS production in TRAPS that is most pronounced in monocytes.

ROS mediate increased MAPK signaling and inflammatory responses in TNFR1 mutant cells

To determine the role of ROS in inflammatory responses to LPS, we measured the effects of ROS inhibition on MAPK activation and cytokine production. We first measured the effect of ROS inhibition on MAPK phosphorylation in cells from normal mice and mice heterozygous for TNFR1 mutations. The free radical scavenger N-acetylcysteine (NAC) neutralizes ROS as they are generated, providing a broad indication of the role of ROS in biological processes. As previously described, TNFR1 mutant MEFs stimulated with LPS exhibited sustained phosphorylation of JNK, p38, and ERK for up to 120 min compared with WT cells, in which activation of these kinases peaked at 30 min, followed by a rapid decline (Simon et al., 2010). Because ROS prevent the dephosphorylation of MAPKs, we reasoned that ROS inhibitors may reduce the abnormally sustained MAPK activation in the setting of TNFR1 mutations. Indeed, NAC effectively reduced the sustained JNK and p38 phosphorylation at the 2-h time point in TNFR1 heterozygous mutant MEFs and, to a lesser extent, in WT MEFs (Fig. 2 A). Phosphorylation of ERK was not as affected by NAC in TNFR1 mutant cells, but we have previously shown that exaggerated cytokine production by TRAPS cells is dependent on p38 and JNK kinases more than ERK family kinases (Simon et al., 2010). Although NAC has been shown to inhibit the activation of both NF-κB and IRF3, we have not seen increased activation of NF-κB or IRF3, or increased production of the IRF3-dependent cytokine CCL5/RANTES in TRAPS (Simon et al., 2010). It is likely that NAC affects all of these signaling pathways, but specifically abrogates TRAPS hyperresponsiveness through effects on pathologically elevated p38 and JNK phosphorylation.

To determine the role of ROS in inflammatory cytokine production, we measured effects of ROS inhibitors on the production of IL-6 by WT and heterozygous TNFR1 mutant MEFs, which overproduce IL-6 when exposed to LPS (Simon et al., 2010). In addition to NAC, we also used DPI, which acts as a competitive inhibitor of flavin-containing cofactors and is a particularly potent inhibitor of NOX enzymes (Holland and Sherratt, 1972). As previously described, C33Y and T50M TNFR1 heterozygous MEFs produce excess IL-6 in response to LPS compared with WT cells (Fig. 2 B). NAC and DPI significantly blocked excess IL-6 production by TNFR1 mutant cells and, interestingly, also effectively blocked IL-6 production in WT cells (Fig. 2 B), suggesting that there is a role for ROS in the normal inflammatory response to LPS. IFN-β, which is expressed independently of MAPK signaling, was neither hyperproduced by TNFR1 mutant MEFs nor reduced by the addition of antioxidants. The role of ROS in IL-6 signaling is transcriptional, as induction of IL-6 mRNA by LPS in WT and TNFR1 mutant cells was also inhibited by NAC and DPI (Fig. 2 C). Neither of these antioxidants significantly affected cell viability (Fig. S2, A and B).

To determine the significance of these findings in human immune cells, we measured the effects of these antioxidants on PBMCs from TRAPS patients and healthy donors. We have previously shown that PBMCs from TRAPS patients produce excess TNF and IL-6 in response to LPS (Simon et al., 2010). NAC and DPI both decreased IL-6, TNF, and IL-10 production in the TRAPS patient cells back to the levels produced by cells from healthy donors, whereas DPI decreased CXCL8/IL-8 production (Fig. 2 D). In addition, both NAC and DPI significantly lowered cytokine production by PBMCs from healthy donors, supporting a role for ROS in physiological LPS-induced inflammation as well. IFN-β and CCL5/RANTES, both activated by IRF3, were unaffected by antioxidant treatment. This suggests that the efficacy of the antioxidants correlates with dependency on MAPKs, as induction of IL-6, TNF, CXCL8/IL-8, and IL-10 are dependent on MAPKs (Scherle et al., 1998; Chi et al., 2006). Collectively, these results strongly implicate ROS in physiological production of cytokines after TLR4 stimulation in normal cells, and in the maintenance of MAPK activity and excess inflammatory cytokine production in cells harboring TRAPS-associated TNFR1 mutations.

ROS generated by NOXs are not required for inflammatory cytokine production in TNFR1 mutant and normal cells

Based on the potency of DPI in the aforementioned experiments, we sought to identify whether NOXs might be the source of ROS responsible for inflammatory cytokine production in normal and TNFR1 mutant cells. NOX2 participates directly in the innate immune response against foreign pathogens and is a major generator of ROS in monocytes, leading us to study NOX2 as a potential candidate for generating the ROS that supports inflammatory cytokine production. Mice with a null allele of the gene involved in X-linked CGD, gp91^{phox}, which encodes the 91-kD subunit of the

oxidase flavocytochrome b_{558}, lack phagocyte superoxide production by NOX2 and have increased susceptibility to infection with *Staphylococcus aureus* and *Aspergillus fumigatus* (Pollock et al., 1995). Despite this immunodeficiency, macrophages from gp91^{phox}-null mice, as well as CGD patients, produce increased inflammatory cytokines in response to sterile innate stimuli such as LPS (Bylund et al., 2007) and have increased neutrophil infiltration in a sterile peritonitis model (Pollock et al., 1995).

To determine whether removal of NOX2-generated ROS would reverse or weaken the hyperinflammatory phenotype in TNFR1 mutant macrophages, we crossed gp91^{phox}-null mice to TNFR1 C33Y heterozygous mice on an isogenic C57BL/6 background. Peritoneal macrophages from all of the mice

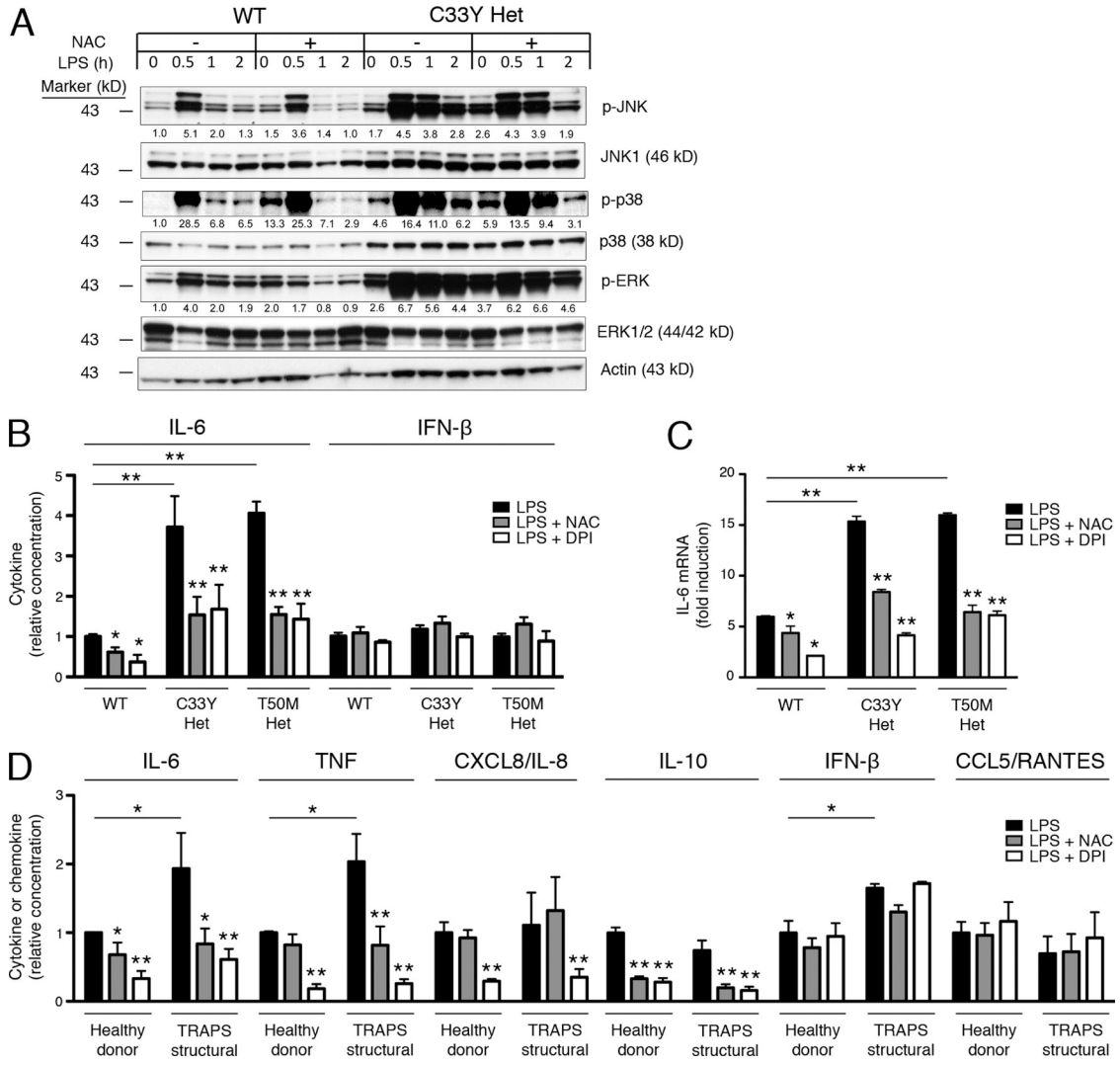

Figure 2. Role of ROS in LPS-induced MAPK activation and cytokine production in normal and TNFR1 mutant cells. (A) WT and C33Y TNFR1 heterozygous MEFs were treated with or without NAC for 30 min, and further treated with LPS for the indicated time, after which JNK, p38, and ERK phosphorylation were measured by Western blot. Numbers shown are the density of each phosphoprotein relative to nonphosphorylated protein, normalized to the WT untreated sample. Actin is included as a loading control. Data are representative of three independent experiments. (B) WT, C33Y TNFR1 heterozygous, and T50M TNFR1 heterozygous MEFs were treated with LPS in the presence of the indicated antioxidants. IL-6 and IFN-β were measured in supernatants. Levels produced by WT MEFs after LPS stimulation ranged from 11.5–104.5 pg/ml (IL-6) and 13.5–23.0 pg/ml (IFN-β; $n = 4$ independent experiments). Data were normalized to the average WT result for each experiment. (C) IL-6 mRNA was measured by qRT-PCR in MEFs of the indicated genotype treated for 6 h with LPS and the indicated antioxidants, as in B. Data are shown as fold induction to LPS (as compared with untreated), and are representative of three experiments. (D) PBMCs from healthy donors ($n = 5$–6) and TRAPS patients with structural mutation ($n = 4$–7) were incubated with LPS and the indicated antioxidants, as in B. IL-6, TNF, CXCL8/IL-8, IL-10, IFN-β, and CCL5/RANTES were measured in supernatants. Levels produced by cells from healthy donors after LPS stimulation ranged from 2.36–9.98 ng/ml (IL-6), 0.21–2.04 ng/ml (TNF), 5.7–77.7 ng/ml (CXCL8/IL-8), 0.054–0.334 ng/ml (IL-10), 0.010–0.058 ng/ml (IFN-β), and 0.138–0.979 ng/ml (CCL5/RANTES; $n = 3$–5 independent experiments). Error bars represent the mean ± SEM. Data were normalized to the average healthy donor result for each experiment. *, $P \leq 0.05$; **, $P < 0.01$.

lacking the gp91^{phox} subunit produced no detectable superoxide after stimulation with PMA (Fig. S3 A). Like the parental strains, heterozygous TNFR1 mutant gp91^{phox}-null mice had no overt phenotype. As previously described (Simon et al., 2010), macrophages from the TNFR1 mutant mice produced more IL-6, TNF, and IL-1β than WT macrophages in response to LPS. Macrophages from gp91^{phox}-null mice produced similar, if not higher, levels of these cytokines as compared with TNFR1 mutant cells, and the hyperresponsiveness seen in TRAPS was not lessened in the absence of NOX2-generated ROS (Fig. 3 A). These results clearly show that NOX2-generated ROS are not required for inflammatory cytokine production by macrophages, in either TRAPS or normal cells.

To determine whether a NOX family member besides NOX2 may be responsible for ROS generation and the subsequent inflammatory sequelae in the CGD model and in TRAPS, we studied NMF333 mice, which harbor a naturally occurring mutation in the p22^{phox} subunit common to NOX1, 2, 3, and 4 (Nakano et al., 2008). After PMA stimulation, macrophages from these mice produced no detectable respiratory burst (Fig. S3 B). However, we discovered that after stimulation with LPS, macrophages from these mice, similar to NOX2-deficient mice, produced elevated levels of IL-6, TNF, and IL-1β (Fig. 3 B) in comparison to isogenic controls. These data show that ROS generated by NOXs containing p22^{phox} are not required for inflammatory cytokine production by macrophages. Interestingly, addition of DPI still strongly blocked the production of inflammatory cytokines in p22^{phox} mutant macrophages (Fig. 3 B). Thus, the antiinflammatory effect of DPI is independent of its effects on NOXs containing p22^{phox}.

ROS have been implicated in the activation of the NLRP3 inflammasome, which results in IL-1β processing and secretion through activation of caspase-1 (Cruz et al., 2007; Zhou et al., 2010a). Thus, we considered that ROS may play a role in IL-6 and TNF production through positive feedback from IL-1β. To determine if this was the case, we tested the response of *Nlrp3*$^{-/-}$, *Casp1*$^{-/-}$, and *Il1r1*$^{-/-}$ macrophages to LPS. As expected, macrophages from *Nlrp3*$^{-/-}$ and *Casp1*$^{-/-}$ mice generated no detectable IL-1β in response to LPS, whereas macrophages from *Il1r1*$^{-/-}$ mice had no defect in IL-1β production. However, LPS-stimulated cells from each of these mice produced normal levels of IL-6 and TNF (Fig. 3 C). Therefore, production of these cytokines in response to LPS is not the result of NLRP3-dependent IL-1β production, nor is it downstream of other NLRP3- or caspase-1–dependent cytokines. Collectively, these data suggest that normal production of inflammatory cytokines other than IL-1β, as well as the increased cytokine responsiveness in TRAPS, is dependent on ROS, but not through effects of ROS on the inflammasome.

Inflammatory cytokine production is linked to mitochondrial ROS production in TRAPS and normal cells

Given that DPI works through the inhibition of flavin-containing enzymes, there are several other ROS generators that may be responsible for producing proinflammatory ROS. In fact, DPI was first identified as an inhibitor of mitochondria (Holland and Sherratt, 1972), as it blocks the flavin components of the electron transport chain. However, DPI was later shown to be less potent as an inhibitor of mitochondrial oxidative phosphorylation than NOX enzymes (Hancock and Jones, 1987) and nitric oxide synthases (Stuehr et al., 1991).

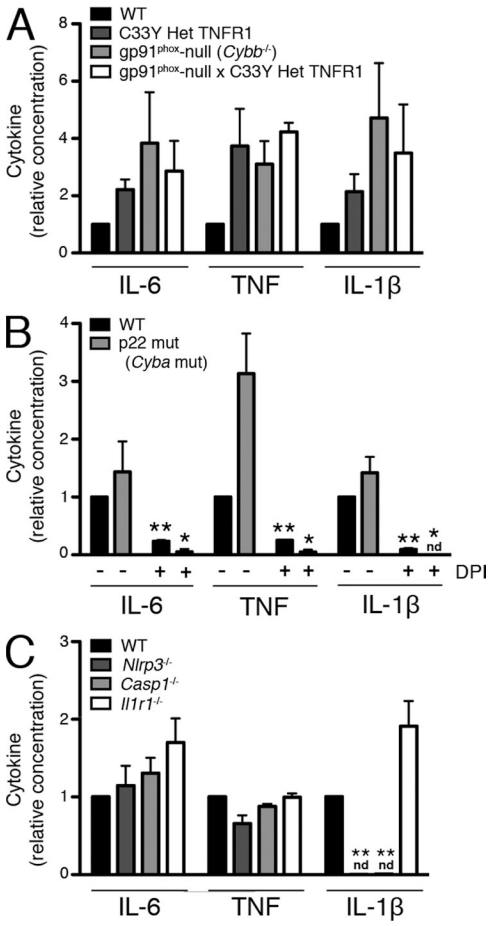

Figure 3. NOX-derived ROS and the inflammasome are not required for LPS-induced cytokine production. (A) Peritoneal macrophages from mice of the indicated genotypes were stimulated with LPS for 6 h, and ATP for the final 15 min, before measuring IL-6, TNF, and IL-1β in the supernatants. Levels produced by WT mice after LPS stimulation ranged from 1.52–1.61 ng/ml (IL-6), 0.23–0.97 ng/ml (TNF), and 0.21–0.46 ng/ml (IL-1β; *n* = 2 independent experiments, 1 mouse in each group). (B) Peritoneal macrophages from mice of the indicated genotypes were incubated with LPS in the presence or absence of DPI for 6 h, and ATP for the final 15 min, before measuring IL-6, TNF, and IL-1β in the supernatants. Levels produced by WT mice after LPS stimulation ranged from 1.52–4.49 ng/ml (IL-6), 0.14–0.19 ng/ml (TNF), and 3.10–4.07 ng/ml (IL-1β; *n* = 3 independent experiments, one mouse in each group). (C) Peritoneal macrophages from mice of the indicated genotypes were stimulated with LPS for 6 h, and ATP for the final 15 min, before measuring IL-6, TNF, and IL-1β in the supernatants. Levels produced by WT mice after LPS stimulation ranged from 1.68–2.70 ng/ml (IL-6), 0.39–0.58 ng/ml (TNF), and 0.18–0.80 ng/ml (IL-1β; *n* = 3 independent experiments, one mouse in each group). nd, not detectable. Error bars represent the mean ± SEM. Data were normalized to the average WT LPS result for each experiment. *, P ≤ 0.05; **, P < 0.01.

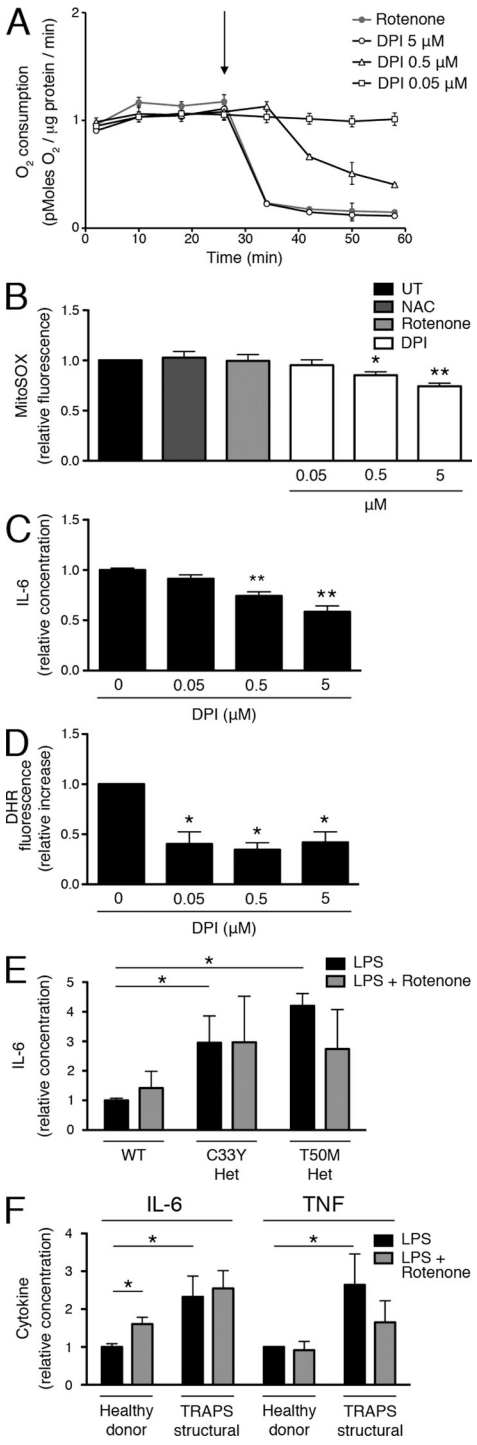

Figure 4. Inhibition of mitochondrial oxygen consumption by DPI. (A) The effect of antioxidants on oxygen consumption rate was measured in WT MEFs with a Seahorse Bioscience XF Analyzer. The arrow indicates time of addition of the antioxidants. A representative plot ($n = 3$) is shown. (B) WT MEFs were incubated with the indicated antioxidants for 1 h or were left untreated and then stained with MitoSOX Red, and ROS levels were determined by flow cytometry. Data were normalized to the untreated result ($n = 3$ independent experiments). (C) WT MEFs were treated with LPS and the indicated concentrations of DPI, after which IL-6 was measured in supernatants. Levels of IL-6 were normalized to the LPS alone result, which ranged from 0.284–0.321 ng/ml ($n = 3$ independent experiments). (D) WT MEFs were treated with PMA and the indicated concentrations of DPI for 1 h. Cells were incubated with DHR, and ROS levels were determined by flow cytometry. Data were normalized to the increase in fluorescence (as compared with untreated) of the PMA alone sample for each experiment ($n = 3$ independent experiments). (E) WT, C33Y TNFR1 heterozygous, and T50M TNFR1 heterozygous MEFs were treated with LPS in the presence or absence of rotenone, after which IL-6 was measured in supernatants. IL-6 levels were normalized to the WT LPS alone result, which ranged from 11.5–104.5 pg/ml ($n = 4$ independent experiments). (F) PBMCs from healthy donors ($n = 6$) and TRAPS patients with structural mutations ($n = 6$) were incubated with LPS in the presence or absence of rotenone, after which IL-6 and TNF were measured in the supernatants. IL-6 and TNF levels were normalized to the healthy donor LPS alone result, which ranged from 1.31–2.28 ng/ml (IL-6) and 0.274–0.661 ng/ml (TNF; $n = 6$ independent experiments). Error bars represent the mean ± SEM.

For this reason, the effects of DPI are most commonly attributed to inhibition of NOX enzymes, even when used at high doses (≥10 μM; Dostert et al., 2008; Martinon et al., 2010; van de Veerdonk et al., 2010). We took advantage of the differential potency of DPI on NOXs and mitochondria to determine the relevant target for its antiinflammatory effects. In intact MEFs, DPI reduced mitochondrial oxygen consumption as effectively as rotenone, a standard blocker of complex I, at the same concentration at which it affects cytokine production (5 μM). Lowering the concentration of DPI reduced its inhibition of oxygen consumption in a dose-dependent manner, with little inhibition below 0.5 μM (Fig. 4 A).

DPI has been shown to block mitochondrial ROS, which are produced as a consequence of electron leak during the electron transport chain (Li and Trush, 1998); it inhibits flavin adenine dinucleotide (FAD), which is present in both complex I (NADH-quinone oxidoreductase) and complex II (succinyl dehydrogenase). Using the MitoSOX Red dye, a probe of mitochondrial superoxide production in live cells, we found that DPI inhibits mitochondrial ROS in the same dose range at which it inhibits oxygen consumption (Fig. 4 B). To correlate these findings with LPS-induced inflammatory cytokine production, we added these same concentrations of DPI to LPS-stimulated MEFs. Concentrations of DPI that inhibited mitochondrial ROS generation also inhibited inflammatory cytokine production in the same dose-dependent manner (Fig. 4 C). At doses down to 0.05 μM, however, DPI was equally effective at inhibiting PMA-induced ROS, which can be attributed to NOX enzymes (Fig. 4 D). These data strongly point to mitochondrial respiration, not NOXs, as the source of ROS involved in LPS-induced inflammatory cytokine production.

Rather than ROS, it is possible that the ATP generated through mitochondrial respiration might be the driving force behind inflammatory responses to LPS. To determine whether this is the case, we used rotenone, an effective electron transport inhibitor (Fig. 4 A). Although rotenone has been shown to both increase and decrease mitochondrial ROS production in a variety of cell types (Li et al., 2003; Thompson et al., 2007),

we found that it does not affect mitochondrial ROS production in MEFs at time points that are relevant to signaling (Fig. 4 B). Overall, rotenone was not effective at blocking inflammatory cytokine production in either MEFs (Fig. 4 E) or human PBMCs (Fig. 4 F), suggesting that an intact electron transport chain is not required for inflammatory cytokine production. These data point to mitochondrial ROS rather than ATP as the proinflammatory signal generated by mitochondria.

Mitochondrial function and mitochondrial ROS production are altered in TRAPS

We reasoned that cells harboring heterozygous TNFR1 mutations associated with TRAPS might exhibit increased basal mitochondrial electron transport and oxidative phosphorylation, which could lead to increased inflammatory responses. Measurement of total ATP levels with a luminol-based reagent showed that heterozygous TNFR1 mutant MEFs (Fig. 5 A) and PBMCs from TRAPS patients with structural TNFR1 mutations (Fig. 5 B) both exhibit a small but significant increase in ATP levels over controls. Measurement of oxygen consumption showed that heterozygous C33Y TNFR1 mutant MEFs have a significantly higher level of basal oxygen consumption, and both C33Y and T50M heterozygous TNFR1 mutant MEFs have significantly increased maximum oxidative capacity measured after addition of the electron transport uncoupler dinitrophenol (Fig. 5, C and D). In support of altered mitochondrial respiration, the mitochondrial membrane potential measured with the potentiometric dye TMRM was increased in TNFR1 mutant MEFs (Fig. 5 E). The higher ATP levels in cells harboring TNFR1 mutations is not caused by a glycolytic source, as the extracellular acidification rate in the TNFR1 mutant MEFs was similar to that of the WT MEFs (Fig. 5 F). Although the increased oxygen consumption observed in TNFR1 mutant cells could be caused by increased mitochondrial content, mitochondrial copy number in TNFR1 mutant MEFs was not significantly different from WT controls (Fig. 5 G). PBMCs from TRAPS patients with structural TNFR1 mutations asymptomatic at the time of sample collection also showed alterations in mitochondrial function; they displayed elevated basal oxygen consumption and increased oxygen consumption after addition of dinitrophenol as compared with healthy controls (Fig. 5 H, I). This suggests that PBMCs containing TNFR1 mutations have a greater capacity for mitochondrial respiration.

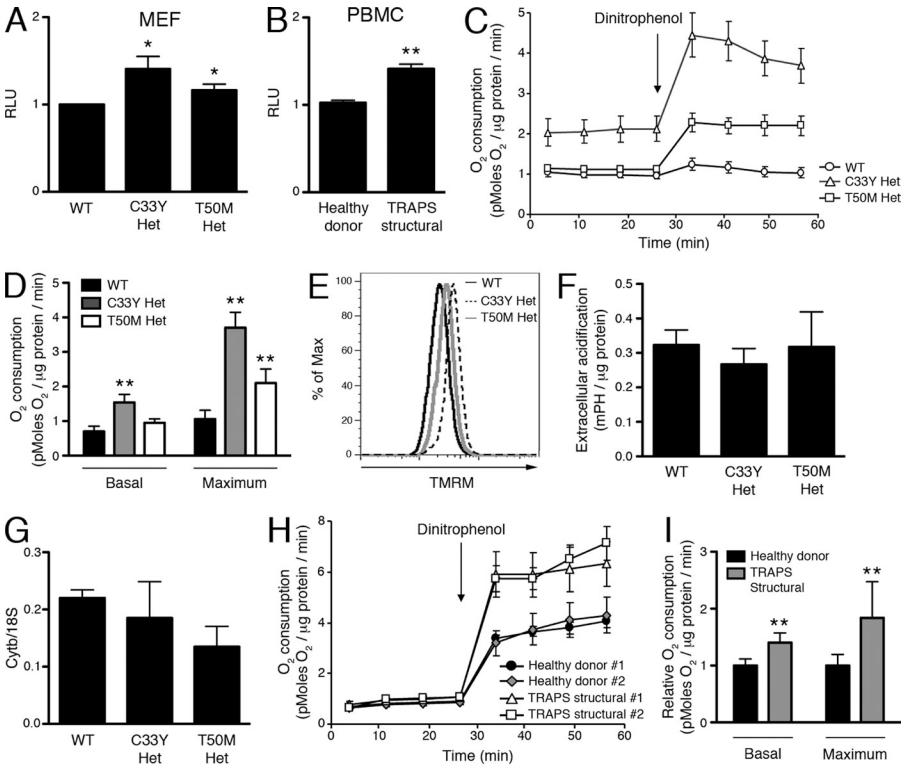

Figure 5. Increased ATP levels and oxidative capacity in cells with TRAPS-associated TNFR1 mutations. (A) ATP level was measured in WT and TNFR1 mutant MEFs. Cell numbers were determined with a CyQuant assay, and data were normalized to the WT result ($n = 5$ independent experiments). RLU, relative luminescence units. (B) ATP level was measured in PBMCs from healthy donors ($n = 8$) and TRAPS patients with structural mutations ($n = 6$). Cell numbers were determined with a CyQuant assay, and data were normalized to the healthy donor result ($n = 4$ independent experiments). RLU, relative luminescence units. (C) Oxygen consumption was measured in WT, C33Y TNFR1 heterozygous, and T50M TNFR1 heterozygous MEFs using the Seahorse Bioscience XF Analyzer. Dinitrophenol was added as indicated by the arrow. A representative plot ($n = 3$) is shown. (D) Basal and maximum oxygen consumption were determined in MEFs of the indicated genotypes using the Seahorse Bioscience XF Analyzer ($n = 3$ independent experiments). (E) TMRM staining of WT, C33Y TNFR1 heterozygous, and T50M TNFR1 heterozygous MEFs was determined by flow cytometry. A representative histogram ($n = 3$) is shown. (F) Extracellular acidification was measured in WT, C33Y TNFR1 heterozygous, and T50M TNFR1 heterozygous MEFs using the Seahorse Bioscience XF Analyzer ($n = 3$ independent experiments). (G) Mitochondrial copy number was measured by qRT-PCR in MEFs of the indicated genotypes. Cytb mitochondrial DNA was compared with 18S genomic DNA ($n = 2$ independent experiments). (H) Oxygen consumption was measured in PBMCs from healthy donors ($n = 10$) and patients with TRAPS structural mutations ($n = 6$) using the Seahorse Bioscience XF Analyzer. Dinitrophenol was added as indicated by the arrow. A representative plot with two healthy donors and two TRAPS patients with structural mutations is shown ($n = 5$ independent experiments). (I) Basal and maximum oxygen consumption were determined from healthy donors ($n = 10$) and TRAPS patients with structural mutations (TRAPS structural; $n = 6$) using the Seahorse Bioscience XF Analyzer. Error bars represent the mean ± SEM. Data were normalized to the average healthy donor result ($n = 5$ independent experiments). *, $P \leq 0.05$; **, $P < 0.01$.

To more directly measure mitochondrial ROS production in cells harboring TNFR1 mutations, we used MitoSOX Red. Unlike DHR, MitoSOX Red staining in MEFs did not increase in response to the NOX-mediated respiratory burst, indicating that the dye is more specific to mitochondrial ROS. In addition, MitoSOX Red staining did not increase in response to LPS stimulation, suggesting that there is not an acute increase in mitochondrial ROS generation during an inflammatory response (Fig. S4 A). Both C33Y and T50M TNFR1 heterozygous mutant MEFs showed significantly higher spontaneous mitochondrial ROS generation than WT MEFs (Fig. 6 A). PBMCs from TRAPS patients with structural TNFR1 mutations, but not TNFR1 polymorphisms, also produced significantly higher mitochondrial ROS than PBMCs from healthy donors (Fig. 6 B). Excess mitochondrial superoxide stimulates increased transcription of MnSOD, a mitochondrial-specific superoxide dismutase (Miao and St Clair, 2009; Pani et al., 2009). To determine if the increased mitochondrial superoxide production measured in TRAPS is sufficient to induce this biological response, we measured MnSOD transcripts in TNFR1 mutant MEFs and PBMCs from patients with TRAPS structural mutations by quantitative RT-PCR (qRT-PCR). We found more than a twofold higher level of MnSOD mRNA at baseline in both of these cell types (Fig. 6, C and D). mRNA of the endogenous antioxidant thioredoxin was slightly higher in PBMCs from TRAPS patients with structural mutations as compared with healthy donors, but not as highly elevated as MnSOD (Fig. 6 D). These data show that TNFR1 mutations in TRAPS stimulate increased mitochondrial oxidative capacity and ROS production, leading to an antioxidant response associated with chronic oxidative stress.

Inhibition of mitochondrial ROS reduces IL-6 production

If mitochondrial ROS play an important role in inflammatory cytokine production, ROS scavengers specific to mitochondrial ROS should block LPS-induced inflammatory cytokine production with particular efficacy. Mitoquinone (MitoQ), a coenzyme Q_{10} analogue that acts as a ROS scavenger, contains a lipophilic triphenylphosphonium cation that causes the antioxidant to accumulate several hundredfold within mitochondria because of the high mitochondrial membrane potential (Murphy and Smith, 2007; Villalba et al., 2010). MitoQ has been shown to effectively decrease mitochondrial ROS levels, both at baseline and after the addition of respiratory chain inhibitors that increase mitochondrial ROS (Chernyak et al., 2006). Decyl-TPP bromide (dTPP), which contains the same lipophilic cation but has no antioxidant activity, was used as a control. Neither MitoQ nor dTPP affected oxygen consumption (Fig. S4 B) or cell viability (Fig. S2, A and B). MitoQ reduced LPS-induced IL-6 production in C33Y and T50M TNFR1 heterozygous MEFs nearly back to the levels secreted by WT cells (Fig. 7 A). However, IFN-β levels were not reduced by the addition of MitoQ (Fig. 7 A). Like DPI, the inhibition of IL-6 production by MitoQ was at the transcriptional level, and inhibition of IL-6 transcription could be seen in WT MEFs as well as TNFR1 mutant cells (Fig. 7 B). Importantly, MitoQ suppressed the production of IL-6, TNF, CXCL8/IL-8, and IL-10 in PBMCs from TRAPS patients back to the levels produced by control cells from healthy donors, and also suppressed the production of these cytokines by cells from healthy donors in response to LPS (Fig. 7 C). IFN-β and CCL5/RANTES production in response to LPS was unaffected by the addition of MitoQ, suggesting that the efficacy of MitoQ is through its action on MAPKs and

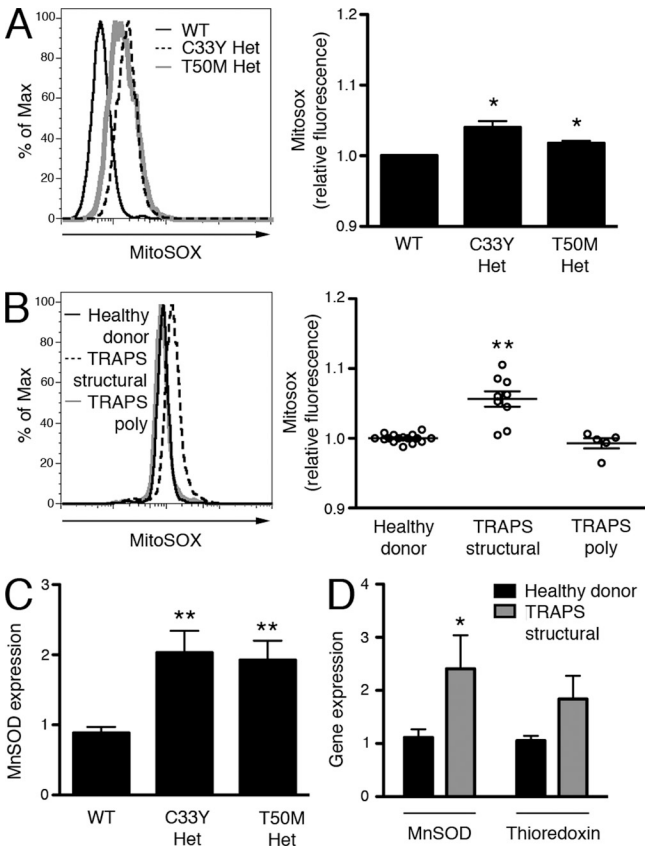

Figure 6. Mitochondrial superoxide production is increased in TRAPS. (A) WT, C33Y TNFR1 heterozygous, and T50M TNFR1 heterozygous MEFs were incubated with MitoSOX Red for 1 h and ROS levels were determined by flow cytometry. Histogram shows representative staining and bar graph shows results of three independent experiments. Data were normalized to the average WT result for each experiment. (B) Monocytes from healthy donors ($n = 15$), TRAPS patients with structural mutations (TRAPS structural; $n = 9$), and TRAPS patients with TNFR1 polymorphisms (TRAPS poly; $n = 5$) were incubated with MitoSOX Red for 1 h, and ROS levels were determined by flow cytometry. Histogram shows representative staining and bar graph shows results of six independent experiments; each symbol represents a unique patient. Data were normalized to the average healthy donor result for each experiment. (C) SOD2 mRNA was measured by qRT-PCR in MEFs of the indicated genotype ($n = 3$ independent experiments). Data represent gene expression relative to β2-microglobulin. (D) SOD2 and thioredoxin mRNA were measured by qRT-PCR in PBMCs from healthy donors ($n = 6–7$) and TRAPS patients with structural mutations ($n = 14$). Data represent gene expression relative to β2-microglobulin. Error bars represent the mean ± SEM. *, $P \leq 0.05$; **, $P < 0.01$.

independent of IRF3. These data identify mitochondrial ROS as an important component of the inflammatory response, both in normal cells and in the hyperresponsiveness of cells harboring TNFR1 mutations in TRAPS.

DISCUSSION

Through the measurement of cellular respiration in intact cells and the use of targeted antioxidants, we demonstrate here that alterations in baseline mitochondrial ROS production can affect LPS-induced cytokine production. We propose a model in which mitochondrial ROS support a balance between MAP kinases and phosphatases that results in the normal inflammatory response. If mitochondrial respiration or ROS production is inhibited, inflammatory cytokine production in response to LPS is blunted. In TRAPS, increased mitochondrial ROS production inactivates MAPK phosphatases and leads to sustained MAPK activity that enhances innate immune responses (Fig. 7 D). Multiple lines of evidence implicate mitochondrial respiration as a source of ROS that supports normal inflammatory responses to LPS and drives hyperinflammation in TRAPS: (a) the concentrations of DPI that block mitochondrial respiration and ROS correlate with its antiinflammatory effects; (b) DPI and MitoQ are the most effective at suppressing inflammatory cytokine production in

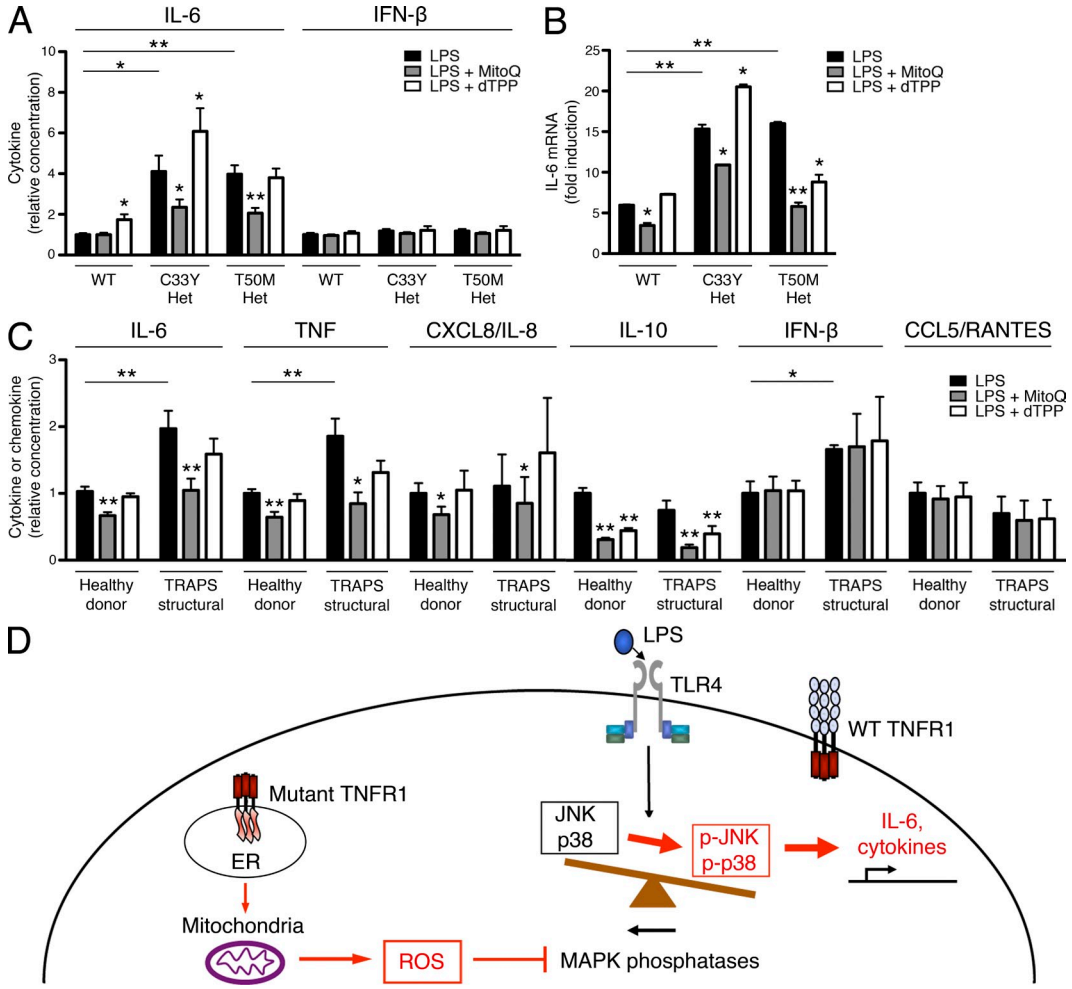

Figure 7. Inhibition of mitochondrial ROS can reduce normal cytokine production and reverse hyperinflammatory responses in TRAPS. (A) WT, C33Y TNFR1 heterozygous, and T50M TNFR1 heterozygous MEFs were treated with LPS in the presence of the mitochondrial ROS scavenger MitoQ and its control, dTPP. IL-6 and IFN-β were measured in supernatants. Levels produced by WT MEFs after LPS stimulation ranged from 11.5–104.5 pg/ml (IL-6) and 13.5–23.0 pg/ml (IFN-β; $n = 3$ independent experiments). (B) IL-6 mRNA was measured by qRT-PCR in MEFs of the indicated genotype treated for 6 h with LPS and the indicated reagents as in A. Data are shown as fold induction to LPS (as compared with untreated), and are representative of three independent experiments. (C) PBMCs from healthy donors ($n = 5–8$) and TRAPS patients with structural mutations (TRAPS structural; $n = 4$) were incubated with LPS and the indicated reagents as in A. IL-6, TNF, CXCL8/IL-8, IL-10, IFN-β, and CCL5/RANTES were measured in supernatants. Levels produced by PBMCs from healthy donors after LPS stimulation ranged from 0.93–8.67 ng/ml (IL-6), 1.17–4.12 ng/ml (TNF), 5.7–77.7 ng/ml (CXCL8/IL-8), 0.054–0.334 ng/ml (IL-10), 0.010–0.058 ng/ml (IFN-β), and 0.138–0.979 ng/ml (CCL5/RANTES; $n = 3–4$ independent experiments). Data were normalized to the average WT or healthy donor LPS result for each experiment. *, $P \leq 0.05$; **, $P < 0.01$. (D) Schematic model of how mitochondrial ROS support LPS hyperresponsiveness in TRAPS.

all cells; (c) rotenone, which suppresses mitochondrial electron transport but not ROS production, is not effective at blocking cytokine production; (d) cells harboring TNFR1 mutations associated with TRAPS have increased basal oxygen consumption, respiratory capacity, and mitochondrial ROS, but respond normally in terms of the NOX-generated respiratory burst; (e) blockade of mitochondrial ROS production in TNFR1 mutant cells specifically reduces hyperresponsiveness to LPS. Mitochondrial ROS may provide an alternate source of ROS that allows normal or enhanced inflammatory responses in the setting of NOX deficiency (van de Loo et al., 2003; Hultqvist et al., 2004; George-Chandy et al., 2008; Meissner et al., 2010; van de Veerdonk et al., 2010) and may explain the associated inflammatory symptoms seen in CGD patients alongside their immunodeficiency (Rosenzweig, 2008).

These results identify mitochondria, which are a major source of physiological cellular ROS (Chance et al., 1979; Balaban et al., 2005), in the genesis of ROS that drive inflammation. Although the effectiveness of DPI is often attributed to inhibition of NOXs, the ability of DPI to block cytokine production in cells devoid of the NOX subunit $p22^{phox}$ suggests that there are other sources of ROS important in the inflammatory response. We show here that DPI is as potent an inhibitor of oxygen consumption as rotenone, which blocks complex I of the electron transport chain. DPI blocks oxygen consumption, mitochondrial ROS generation, and IL-6 production in a similar dose–response manner. Thus, DPI appears to exert its antiinflammatory effects through blockade of mitochondrial respiration. Moreover, many of the functions ascribed to NOXs in inflammation because of the use of flavin inhibitors such as DPI may actually be caused by mitochondria or other ROS-generating pathways. In support of this concept, Rho zero L929 cells that lack mitochondrial DNA and an intact mitochondrial respiratory chain have decreased production of IL-6 in response to TNF, although these results must be interpreted with caution given the dramatic metabolic changes in these cells (Schulze-Osthoff et al., 1993). Our data showing that MitoQ blocks transcription of inflammatory cytokines implicates mitochondrial ROS in this process. The increased MnSOD expression we find in TNFR1 mutant cells is an indicator of chronic oxidative stress (Miao and St Clair, 2009; Pani et al., 2009) that may feed back and cause even more dysregulated inflammation.

Several mechanisms may allow mutant TNFR1 to enhance oxygen consumption and ROS production. The endoplasmic reticulum, where mutant TNFR1 resides, can provide signals to activate mitochondrial respiration, including a calcium signal transduced by mitochondrial InsP3 receptors (Cárdenas et al., 2010). Mutant TNFR1 may increase activation of riboflavin kinase, which can associate with TNFR1 (Yazdanpanah et al., 2009), leading to enhanced charging of FAD-dependent enzymes in the mitochondria. Another potential mechanism could involve low-level activation of ER stress signaling involving XBP-1, which has been shown to induce hyperresponsiveness to TLR stimulation reminiscent of what is seen in TRAPS. Although expression of the ER stress–induced proteins BiP and CHOP appear normal in cells from TRAPS mice and patients (Simon et al., 2010), macrophages undergoing ER stress can exhibit increased XBP-1 splicing without activation of many ER stress–induced genes (Martinon et al., 2010). In addition, TNFR1 has been shown to sense ER stress and mediate ER stress–induced JNK activation (Yang et al., 2006). Chronic ER stress or enhanced ER stress sensing in the setting of TNFR1 mutations could activate proinflammatory signaling pathways in a ROS-dependent fashion. Future research should more specifically address the mechanisms by which TNFR1 mutations enhance mitochondrial respiration.

Although the genetic mutations and defective trafficking of the mutant TNFR1 protein have been identified in TRAPS, current treatments, including TNF blockade, do not adequately control the symptoms of many TRAPS patients or prevent amyloidosis (Hull et al., 2002; Church et al., 2006). Our findings identify mitochondrial ROS as a driver of inflammation in TRAPS and potentially other autoinflammatory diseases. In addition, the identification of mitochondria as a source of ROS contributing to LPS responsiveness in healthy cells has broad implications for future studies on the role of ROS in inflammatory responses by the normal immune system. Although it has recently been shown that mitochondrial damage and inhibition of mitophagy can activate the NLRP3 inflammasome and IL-1β cleavage in a ROS-dependent manner (Zhou et al., 2010b), our results suggest a more general role for mitochondrial ROS in the induction of inflammatory cytokines upstream of inflammasome activation. In TRAPS, increased mitochondrial ROS results from enhanced oxidative phosphorylation. Whether the increased ROS observed in cells from patients with autoinflammatory disease associated with NLRP3 mutations (Tassi et al., 2010) also originates from mitochondria is not yet known. Blockade of ROS production by mitochondria provides a new therapeutic strategy to decrease symptoms in TRAPS and other inflammatory states.

MATERIALS AND METHODS

Patient samples. Patients and controls were included in this study after informed consent under the approved clinical research protocol NIAMS 94-AR-0105. TRAPS patients with structural mutations were heterozygous for structural TRAPS-associated mutations in *Tnfrsf1A* (H22Y, C33Y, T50M, C33G, C52G, C52F, C30Y, or del c.193-14). Patients with nonstructural TNFR1 mutations were heterozygous for *Tnfrsf1A* R92Q or P46L mutations. PBMCs were collected by density centrifugation using Ficoll-Paque PLUS (GE Healthcare), with PBMCs collected at the interface.

Mice and MEFs. TNFR1 mutant mice have been previously described (Simon et al., 2010) and were used on the C57BL/6 background. $gp91^{phox}$-null mice on the C57BL/6 background (B6.129S-*Cybb*^{tm1Din}/J; The Jackson Laboratory) were crossed to TRAPS C33Y mutant mice to generate mice containing both mutations. Presence of the heterozygous mutant TNFR1 allele and absence of the $gp91^{phox}$ allele was confirmed by genotyping. NMF333 ($p22^{phox}$ mutant) mice (A.B6 *Tyr*$^{+}$-*Cyba*^{nmf333}/J; The Jackson Laboratory) were compared with their isogenic control, AJ.Tyr mice (A.B6-*Tyr*$^{+}$/J; The Jackson Laboratory). MEFs were generated from embryonic day 12–13 embryos of each genotype following established protocols. *Nlrp3*$^{-/-}$ mice were provided by V. Dixit (Genentech, South San Francisco, CA),

Casp1$^{-/-}$ mice were provided by R. Flavell (Yale University, New Haven, CT), and *Il1r*$^{-/-}$ mice were purchased from The Jackson Laboratory (B6.129S7-*Il1r1*^{tm1Imx}/J). All animal procedures in mice were performed according to approved National Institute of Arthritis and Musculoskeletal and Skin Diseases animal protocols.

Cell stimulation and cytokine assays. PBMCs were incubated at 10^6 cells/ml in a 96-well plate in RPMI medium plus 10% heat-inactivated FCS. MEFs were plated in a 96-well plate at 10^6 cells/ml in DMEM medium plus 10% heat-inactivated FCS. Mouse peritoneal macrophages were collected by established methods from unmanipulated mice and plated at 10^6 cells/ml in a 96-well plate in RPMI medium plus 10% heat-inactivated FCS. Cells were allowed to adhere for 30 min in serum-free RPMI medium, followed by a wash. All cells were incubated with or without LPS (Ultrapure *Salmonella minnesota* R595; List Biological Laboratories Inc.) at 100 ng/ml (MEFs and peritoneal macrophages) or 10 ng/ml (PBMCs). After 6 h, supernatant was collected, centrifuged to remove cells and debris, and stored at −80°C for later analysis. In mouse peritoneal macrophages, 5 mM ATP (Sigma-Aldrich) was added for the last 15 min of incubation. IL-6 cytokine analysis was performed by ELISA using DuoSet ELISA kits (R&D Systems) for mouse and human IL-6. IFN-β cytokine analysis was performed by ELISA using VeriKine kits for mouse and human IFN-β (PBL Interferon Source). IL-1β, TNF, CXCL8/IL-8, IL-10, and CCL5/RANTES cytokine analysis was performed using a Bio-Plex Pro Bead Array (Bio-Rad Laboratories). Results were normalized to cell number, as determined by the CyQuant cell proliferation assay (Invitrogen). The following inhibitors were obtained from Sigma-Aldrich and used at the following final concentrations: NAC 10 mM, rotenone 10 μM, DPI 5 μM, or as indicated. MitoQ and decylTPP were obtained from Antipodean Pharmaceuticals and used at 1 μM final concentration.

ROS detection. For DHR-based flow cytometric detection of intracellular ROS, whole blood was subjected to ACK lysis and washed. Cells were then incubated for five minutes with catalase (Sigma-Aldrich), DHR (Sigma-Aldrich), and HBSS buffer with Ca^{2+} and Mg^{2+} and without phenol red. The indicated stimulation was added for 1 h and cells were analyzed on a FACSCalibur flow cytometer (BD). Monocyte and neutrophil subsets were determined on the basis of size and granularity. Mean channel fluorescence was converted to absolute fluorescence using an inverse log transformation and normalized to the untreated WT or healthy donor cells.

For diogenes chemiluminescent detection of superoxide production, PBMCs and neutrophils were collected by double-density centrifugation using Ficoll 1119 and 1077 with PBMCs collected at the top interface and neutrophils at the bottom interface. Cells were seeded in HBSS with Ca^{2+} and Mg^{2+}, and transferred to a 96-well white opaque plate at a concentration of 10^6 cells/ml for PBMCs, and 0.2×10^6 cells/ml for neutrophils. The diogenes reagents (National Diagnostics) were applied to the wells as per the manufacturer's protocol, and 1 μg/ml PMA was immediately added to the samples. Luminescence was measured on a Wallac Victor2 (Perkin Elmer) microplate reader for 90 min. The area under the curve was used to determine cumulative ROS production, and data are presented as the total ROS generation relative to the mean of the healthy adult controls during a given experiment.

For MitoSOX Red–based flow cytometric detection of mitochondrial superoxide, PBMCs were isolated with Ficoll-Paque PLUS (GE Healthcare), and ACK lysis was performed to remove red blood cells. Cells were then incubated with MitoSOX Red superoxide indicator (Invitrogen) for 30 min and washed, and the indicated stimulation (PMA 1 μg/ml or LPS 1 μg/ml) or antioxidants (NAC 10 mM, Rotenone 10 μM, or DPI as indicated) was added for 1 h before cells were analyzed on a FACSCalibur (BD). The monocyte subset was identified on the basis of size and granularity. Mean channel fluorescence was converted to absolute fluorescence using an inverse log transformation and normalized to the untreated WT or healthy donor cells.

Western blot analyses. Cells were lysed in buffer containing 50 mM Tris, pH 7.4, 0.5% Triton X-100, 300 mM NaCl, 2 mM EDTA, 0.4 mM sodium vanadate, and protease inhibitor cocktail (Roche). 40 μg of total protein was applied to each lane and subjected to SDS-PAGE and Western blotting via enhanced chemiluminescence (GE Healthcare). The following primary antibodies were used: JNK1 (554286; BD), phospho-JNK (Thr183/Tyr185, 9251), phospho-p38Thr180/Tyr182 (9215), phospho-ERK Thr202/Tyr204 (9101), p38 (9212), ERK (9102) from Cell Signaling Technology. Multiple exposures were taken to select images with density within the dynamic range using Fuji Image Reader LAS-3000 software and band intensity was quantified using Multi Gauge software (Fujifilm Global). Bands of interest were normalized to the corresponding nonphosphorylated bands as indicated.

qRT-PCR. Total RNA was isolated from cells using RNeasy Mini kit (QIAGEN). First-strand cDNA was prepared using TaqMan Reverse Transcription kit (Applied Biosystems). Equal amounts of cDNA were subjected to PCR to quantitate IL-6 (Mm00446190_m1), SOD2 (mouse, Mm00449726_m1; human, Hs00167309_m1), and TXN (Hs00828652_m1) gene expression with the use of an ABI PRISM 7700 sequence-detection system. Predesigned primer/probe sets for each gene were purchased from Applied Biosystems. Probes specific for β2-microglobulin (mouse, Mm00437762_m1; human, Hs00187842) were used as internal controls. Each measurement in WT MEFs or healthy donors without treatment was normalized to expression of β2-microglobulin (ΔCt). For experiments incorporating treatments, measurements of untreated and treated cells were compared (ΔΔCt). The inverse log of the ΔΔCt was then calculated to give the relative fold change.

ATP level determination. ATP levels were determined using the Cell Titer-Glo luminol assay (Promega). Cells were plated in triplicate at 0.15×10^6 cells/ml (MEFs) or 0.25×10^6 cells/ml (PBMCs) in sterile, white, opaque 96-well plates and incubated for 6 h. Assay was performed according to the manufacturer's instructions. ATP level was calculated in relation to cell number, as determined in parallel by the CyQuant Cell Proliferation Assay kit (Invitrogen).

Seahorse XF-24 metabolic flux analysis. Oxygen consumption rate and extracellular acidification rate were measured at 37°C using an XF24 extracellular analyzer (Seahorse Bioscience). MEFs were seeded in 24-well plates for 24 h and human cells were treated with CELL-TAK (BD) for 30 min. Cells were changed to unbuffered DMEM (DMEM supplemented with 25 mM glucose, 1 mM sodium pyruvate, 31 mM NaCl, 2 mM GlutaMax, pH 7.4) and incubated at 37°C in a non-CO_2 incubator for 1 h All injection reagents were adjusted to pH 7.4 on the day of the assay. Four baseline measurements were taken before sequential injection of mitochondrial inhibitors and antioxidants. Four readings were taken after each addition of dinitrophenol (100 μM), DPI (5 μM or as indicated), rotenone (2 μM), MitoQ (1 μM), or dTPP (1 μM). Oxygen consumption rate and extracellular acidification rate were automatically calculated by the Seahorse XF-24 software. Every point represents an average of 3–6 different wells. After the assays, plates were saved and protein concentration in each well was determined using a BCA assay (Thermo Fisher Scientific).

Mitochondrial membrane potential. Mitochondrial membrane potential was measured by TMRM staining (Invitrogen). MEFs were incubated with 200 nM TMRM for 15 min and then analyzed for fluorescence on a FACSCalibur flow cytometer (BD).

Mitochondrial DNA copy measurement. DNA was collected from WT and TNFR1 mutant MEFs using the Puregene core kit (QIAGEN). Real-time PCR was performed for cytochrome *b* (Cytb) and for nuclease-encoded 18S using SYBR green PCR Master Mix (Applied Biosystems) and the MJ research DNA Engine Opticon 2 fluorescence detection system (Bio-Rad Laboratories). Absolute Cytb DNA copies were normalized to the nuclear gene, 18S. Cytb, forward 5′-CTTTGGGTCCCTTCTAGGAGTCTG-3′, reverse 5′- CGAAGAATCGGGTCAAGGTGGC-3′; 18S, forward 5′-CTTAGAGGGACAAGTGGCGTTC-3′, reverse 5′-CGCTGAGCCAGTCAGTGTAG-3′.

Cell viability. Cell viability was determined using the CyQuant Cell Proliferation Assay (Invitrogen) according to the manufacturer's instructions. Fluorescence was measured on a Wallac Victor2 (Perkin Elmer) microplate reader.

Statistical analysis. Statistical significance was determined by an unpaired two-tailed Student's *t* test, or when appropriate a two-tailed paired Student's *t* test (Fig. 1 A and Fig. 6 A) or two-tailed Mann Whitney test (Fig. 1, B and C, and Fig. 6 B). Statistical analyses were performed using Prism 5 for Mac OS X software (GraphPad Software, Inc.). Where indicated, data from each individual experiment were normalized to the mean WT (MEFs or peritoneal macrophages) or healthy donor (PBMCs) result for that particular experiment. Normalized data from multiple experiments were then compiled to generate cumulative figures in which results are presented as relative data. Data are expressed as mean ± SEM.

Online supplemental material. Fig. S1 shows the ROS responsiveness of human PBMCs to PMA and LPS and clinical correlates of ROS levels in TRAPS. Fig. S2 shows the effects of various antioxidants on cell viability. Fig. S3 shows the ability of macrophages from mice in Fig. 3 (A and B) to generate the respiratory burst in response to PMA stimulation. Fig. S4 shows the mitochondrial ROS responsiveness of MEFs to PMA and the effect of MitoQ and dTPP on oxygen consumption in MEFs. Online supplemental material is available at http://www.jem.org/cgi/content/full/jem.20102049/DC1.

We would like to thank Botond Banfi for NMF333 mice, Richard Flavell for caspase-1–deficient mice, Vishva Dixit for NLRP3-deficient mice, and Jae Jin Chae and Anthony Cruz for assistance with experiments. We would also like to thank Ann Jones, John Ryan, and Ivona Aksentievich for provision of clinical samples, Antipodean Pharmaceuticals for providing MitoQ, and Mike Murphy, Julie Blander, Richard Youle, Harry Malech, Thomas Leto, Narda Whiting-Theobald, and Toren Finkel for helpful discussions and advice.

This research was supported by intramural research funding from National Institute of Arthritis and Musculoskeletal and Skin Diseases. A.C. Bulua was supported by the National Institutes of Health Clinical Research Training Program, a public–private partnership between the Foundation for the National Institutes of Health and Pfizer Inc.

The authors have no competing financial interests.

Submitted: 28 September 2010
Accepted: 12 January 2011

REFERENCES

Balaban, R.S., S. Nemoto, and T. Finkel. 2005. Mitochondria, oxidants, and aging. *Cell*. 120:483–495. doi:10.1016/j.cell.2005.02.001

Burek, C.L., and N.R. Rose. 2008. Autoimmune thyroiditis and ROS. *Autoimmun. Rev.* 7:530–537. doi:10.1016/j.autrev.2008.04.006

Bylund, J., K.L. MacDonald, K.L. Brown, P. Mydel, L.V. Collins, R.E. Hancock, and D.P. Speert. 2007. Enhanced inflammatory responses of chronic granulomatous disease leukocytes involve ROS-independent activation of NF-kappa B. *Eur. J. Immunol.* 37:1087–1096. doi:10.1002/eji.200636651

Capasso, M., M.K. Bhamrah, T. Henley, R.S. Boyd, C. Langlais, K. Cain, D. Dinsdale, K. Pulford, M. Khan, B. Musset, et al. 2010. HVCN1 modulates BCR signal strength via regulation of BCR-dependent generation of reactive oxygen species. *Nat. Immunol.* 11:265–272. doi:10.1038/ni.1843

Cárdenas, C., R.A. Miller, I. Smith, T. Bui, J. Molgó, M. Müller, H. Vais, K.H. Cheung, J. Yang, I. Parker, et al. 2010. Essential regulation of cell bioenergetics by constitutive InsP3 receptor Ca2+ transfer to mitochondria. *Cell*. 142:270–283. doi:10.1016/j.cell.2010.06.007

Chance, B., H. Sies, and A. Boveris. 1979. Hydroperoxide metabolism in mammalian organs. *Physiol. Rev.* 59:527–605.

Chen, J., A.M. Gusdon, T.C. Thayer, and C.E. Mathews. 2008. Role of increased ROS dissipation in prevention of T1D. *Ann. N. Y. Acad. Sci.* 1150:157–166. doi:10.1196/annals.1447.045

Chernyak, B.V., D.S. Izyumov, K.G. Lyamzaev, A.A. Pashkovskaya, O.Y. Pletjushkina, Y.N. Antonenko, D.V. Sakharov, K.W. Wirtz, and V.P. Skulachev. 2006. Production of reactive oxygen species in mitochondria of HeLa cells under oxidative stress. *Biochim. Biophys. Acta.* 1757:525–534. doi:10.1016/j.bbabio.2006.02.019

Chi, H., S.P. Barry, R.J. Roth, J.J. Wu, E.A. Jones, A.M. Bennett, and R.A. Flavell. 2006. Dynamic regulation of pro- and anti-inflammatory cytokines by MAPK phosphatase 1 (MKP-1) in innate immune responses. *Proc. Natl. Acad. Sci. USA*. 103:2274–2279. doi:10.1073/pnas.0510965103

Church, L.D., S.M. Churchman, P.N. Hawkins, and M.F. McDermott. 2006. Hereditary auto-inflammatory disorders and biologics. *Springer Semin. Immunopathol.* 27:494–508. doi:10.1007/s00281-006-0015-6

Cruz, C.M., A. Rinna, H.J. Forman, A.L. Ventura, P.M. Persechini, and D.M. Ojcius. 2007. ATP activates a reactive oxygen species-dependent oxidative stress response and secretion of proinflammatory cytokines in macrophages. *J. Biol. Chem.* 282:2871–2879. doi:10.1074/jbc.M608083200

Dostert, C., V. Pétrilli, R. Van Bruggen, C. Steele, B.T. Mossman, and J. Tschopp. 2008. Innate immune activation through Nalp3 inflammasome sensing of asbestos and silica. *Science*. 320:674–677. doi:10.1126/science.1156995

Filippin, L.I., R. Vercelino, N.P. Marroni, and R.M. Xavier. 2008. Redox signalling and the inflammatory response in rheumatoid arthritis. *Clin. Exp. Immunol.* 152:415–422. doi:10.1111/j.1365-2249.2008.03634.x

George-Chandy, A., I. Nordström, E. Nygren, I.M. Jonsson, J. Postigo, L.V. Collins, and K. Eriksson. 2008. Th17 development and autoimmune arthritis in the absence of reactive oxygen species. *Eur. J. Immunol.* 38:1118–1126. doi:10.1002/eji.200737348

Gilgun-Sherki, Y., E. Melamed, and D. Offen. 2004. The role of oxidative stress in the pathogenesis of multiple sclerosis: the need for effective antioxidant therapy. *J. Neurol.* 251:261–268. doi:10.1007/s00415-004-0348-9

Goldbach-Mansky, R., N.J. Dailey, S.W. Canna, A. Gelabert, J. Jones, B.I. Rubin, H.J. Kim, C. Brewer, C. Zalewski, E. Wiggs, et al. 2006. Neonatal-onset multisystem inflammatory disease responsive to interleukin-1beta inhibition. *N. Engl. J. Med.* 355:581–592. doi:10.1056/NEJMoa055137

Hancock, J.T., and O.T. Jones. 1987. The inhibition by diphenyleneiodonium and its analogues of superoxide generation by macrophages. *Biochem. J.* 242:103–107.

Hoffman, H.M., S. Rosengren, D.L. Boyle, J.Y. Cho, J. Nayar, J.L. Mueller, J.P. Anderson, A.A. Wanderer, and G.S. Firestein. 2004. Prevention of cold-associated acute inflammation in familial cold autoinflammatory syndrome by interleukin-1 receptor antagonist. *Lancet*. 364:1779–1785. doi:10.1016/S0140-6736(04)17401-1

Holland, P.C., and H.S. Sherratt. 1972. Biochemical effects of the hypoglycaemic compound diphenyleneiodonnium. Catalysis of anion-hydroxyl ion exchange across the inner membrane of rat liver mitochondria and effects on oxygen uptake. *Biochem. J.* 129:39–54.

Hull, K.M., E. Drewe, I. Aksentijevich, H.K. Singh, K. Wong, E.M. McDermott, J. Dean, R.J. Powell, and D.L. Kastner. 2002. The TNF receptor-associated periodic syndrome (TRAPS): emerging concepts of an autoinflammatory disorder. *Medicine (Baltimore)*. 81:349–368. doi:10.1097/00005792-200209000-00002

Hultqvist, M., P. Olofsson, J. Holmberg, B.T. Bäckström, J. Tordsson, and R. Holmdahl. 2004. Enhanced autoimmunity, arthritis, and encephalomyelitis in mice with a reduced oxidative burst due to a mutation in the Ncf1 gene. *Proc. Natl. Acad. Sci. USA*. 101:12646–12651. doi:10.1073/pnas.0403831101

Kamata, H., S. Honda, S. Maeda, L. Chang, H. Hirata, and M. Karin. 2005. Reactive oxygen species promote TNFalpha-induced death and sustained JNK activation by inhibiting MAP kinase phosphatases. *Cell*. 120:649–661. doi:10.1016/j.cell.2004.12.041

Kanayama, A., and Y. Miyamoto. 2007. Apoptosis triggered by phagocytosis-related oxidative stress through FLIPS down-regulation and JNK activation. *J. Leukoc. Biol.* 82:1344–1352. doi:10.1189/jlb.0407259

Lambeth, J.D. 2004. NOX enzymes and the biology of reactive oxygen. *Nat. Rev. Immunol.* 4:181–189. doi:10.1038/nri1312

Landmesser, U., S. Dikalov, S.R. Price, L. McCann, T. Fukai, S.M. Holland, W.E. Mitch, and D.G. Harrison. 2003. Oxidation of tetrahydrobiopterin leads to uncoupling of endothelial cell nitric oxide synthase in hypertension. *J. Clin. Invest.* 111:1201–1209.

Li, Y., and M.A. Trush. 1998. Diphenyleneiodonium, an NAD(P)H oxidase inhibitor, also potently inhibits mitochondrial reactive oxygen species production. *Biochem. Biophys. Res. Commun.* 253:295–299. doi:10.1006/bbrc.1998.9729

Li, N., K. Ragheb, G. Lawler, J. Sturgis, B. Rajwa, J.A. Melendez, and J.P. Robinson. 2003. Mitochondrial complex I inhibitor rotenone induces apoptosis through enhancing mitochondrial reactive oxygen species production. *J. Biol. Chem.* 278:8516–8525. doi:10.1074/jbc.M210432200

Lobito, A.A., F.C. Kimberley, J.R. Muppidi, H. Komarow, A.J. Jackson, K.M. Hull, D.L. Kastner, G.R. Screaton, and R.M. Siegel. 2006. Abnormal disulfide-linked oligomerization results in ER retention and altered signaling by TNFR1 mutants in TNFR1-associated periodic fever syndrome (TRAPS). *Blood.* 108:1320–1327. doi:10.1182/blood-2005-11-006783

Martinon, F., X. Chen, A.H. Lee, and L.H. Glimcher. 2010. TLR activation of the transcription factor XBP1 regulates innate immune responses in macrophages. *Nat. Immunol.* 11:411–418. doi:10.1038/ni.1857

Meissner, F., R.A. Seger, D. Moshous, A. Fischer, J. Reichenbach, and A. Zychlinsky. 2010. Inflammasome activation in NADPH oxidase defective mononuclear phagocytes from patients with chronic granulomatous disease. *Blood.* 116:1570–1573. doi:10.1182/blood-2010-01-264218

Meng, T.C., T. Fukada, and N.K. Tonks. 2002. Reversible oxidation and inactivation of protein tyrosine phosphatases in vivo. *Mol. Cell.* 9:387–399. doi:10.1016/S1097-2765(02)00445-8

Miao, L., and D.K. St Clair. 2009. Regulation of superoxide dismutase genes: implications in disease. *Free Radic. Biol. Med.* 47:344–356. doi:10.1016/j.freeradbiomed.2009.05.018

Morgenstern, D.E., M.A. Gifford, L.L. Li, C.M. Doerschuk, and M.C. Dinauer. 1997. Absence of respiratory burst in X-linked chronic granulomatous disease mice leads to abnormalities in both host defense and inflammatory response to *Aspergillus fumigatus*. *J. Exp. Med.* 185:207–218. doi:10.1084/jem.185.2.207

Murphy, M.P., and R.A. Smith. 2007. Targeting antioxidants to mitochondria by conjugation to lipophilic cations. *Annu. Rev. Pharmacol. Toxicol.* 47:629–656. doi:10.1146/annurev.pharmtox.47.120505.105110

Nakano, Y., C.M. Longo-Guess, D.E. Bergstrom, W.M. Nauseef, S.M. Jones, and B. Bánfi. 2008. Mutation of the Cyba gene encoding p22phox causes vestibular and immune defects in mice. *J. Clin. Invest.* 118:1176–1185.

Nathan, C. 2003. Specificity of a third kind: reactive oxygen and nitrogen intermediates in cell signaling. *J. Clin. Invest.* 111:769–778.

Nathan, C. 2006. Neutrophils and immunity: challenges and opportunities. *Nat. Rev. Immunol.* 6:173–182. doi:10.1038/nri1785

Pani, G., O.R. Koch, and T. Galeotti. 2009. The p53-p66shc-Manganese Superoxide Dismutase (MnSOD) network: a mitochondrial intrigue to generate reactive oxygen species. *Int. J. Biochem. Cell Biol.* 41:1002–1005. doi:10.1016/j.biocel.2008.10.011

Pétrilli, V., S. Papin, C. Dostert, A. Mayor, F. Martinon, and J. Tschopp. 2007. Activation of the NALP3 inflammasome is triggered by low intracellular potassium concentration. *Cell Death Differ.* 14:1583–1589. doi:10.1038/sj.cdd.4402195

Pollock, J.D., D.A. Williams, M.A. Gifford, L.L. Li, X. Du, J. Fisherman, S.H. Orkin, C.M. Doerschuk, and M.C. Dinauer. 1995. Mouse model of X-linked chronic granulomatous disease, an inherited defect in phagocyte superoxide production. *Nat. Genet.* 9:202–209. doi:10.1038/ng0295-202

Ravet, N., S. Rouaghe, C. Dodé, J. Bienvenu, J. Stirnemann, P. Lévy, M. Delpech, and G. Grateau. 2006. Clinical significance of P46L and R92Q substitutions in the tumour necrosis factor superfamily 1A gene. *Ann. Rheum. Dis.* 65:1158–1162. doi:10.1136/ard.2005.048611

Reth, M. 2002. Hydrogen peroxide as second messenger in lymphocyte activation. *Nat. Immunol.* 3:1129–1134. doi:10.1038/ni1202-1129

Rosenzweig, S.D. 2008. Inflammatory manifestations in chronic granulomatous disease (CGD). *J. Clin. Immunol.* 28:S67–S72. doi:10.1007/s10875-007-9160-5

Scherle, P.A., E.A. Jones, M.F. Favata, A.J. Daulerio, M.B. Covington, S.A. Nurnberg, R.L. Magolda, and J.M. Trzaskos. 1998. Inhibition of MAP kinase kinase prevents cytokine and prostaglandin E2 production in lipopolysaccharide-stimulated monocytes. *J. Immunol.* 161:5681–5686.

Schmidt, H.H. 1992. NO., CO and. OH. Endogenous soluble guanylyl cyclase-activating factors. *FEBS Lett.* 307:102–107. doi:10.1016/0014-5793(92)80910-9

Schulze-Osthoff, K., R. Beyaert, V. Vandevoorde, G. Haegeman, and W. Fiers. 1993. Depletion of the mitochondrial electron transport abrogates the cytotoxic and gene-inductive effects of TNF. *EMBO J.* 12:3095–3104.

Sellak, H., E. Franzini, J. Hakim, and C. Pasquier. 1994. Reactive oxygen species rapidly increase endothelial ICAM-1 ability to bind neutrophils without detectable upregulation. *Blood.* 83:2669–2677.

Sevier, C.S., and C.A. Kaiser. 2008. Ero1 and redox homeostasis in the endoplasmic reticulum. *Biochim. Biophys. Acta.* 1783:549–556. doi:10.1016/j.bbamcr.2007.12.011

Shiloh, M.U., J.D. MacMicking, S. Nicholson, J.E. Brause, S. Potter, M. Marino, F. Fang, M. Dinauer, and C. Nathan. 1999. Phenotype of mice and macrophages deficient in both phagocyte oxidase and inducible nitric oxide synthase. *Immunity.* 10:29–38. doi:10.1016/S1074-7613(00)80004-7

Simon, A., H. Park, R. Maddipati, A.A. Lobito, A.C. Bulua, A.J. Jackson, J.J. Chae, R. Ettinger, H.D. de Koning, A.C. Cruz, et al. 2010. Concerted action of wild-type and mutant TNF receptors enhances inflammation in TNF receptor 1-associated periodic fever syndrome. *Proc. Natl. Acad. Sci. USA.* 107:9801–9806. doi:10.1073/pnas.0914118107

Stuehr, D.J., O.A. Fasehun, N.S. Kwon, S.S. Gross, J.A. Gonzalez, R. Levi, and C.F. Nathan. 1991. Inhibition of macrophage and endothelial cell nitric oxide synthase by diphenyleneiodonium and its analogs. *FASEB J.* 5:98–103.

Tagen, M., A. Elorza, D. Kempuraj, W. Boucher, C.L. Kepley, O.S. Shirihai, and T.C. Theoharides. 2009. Mitochondrial uncoupling protein 2 inhibits mast cell activation and reduces histamine content. *J. Immunol.* 183:6313–6319. doi:10.4049/jimmunol.0803422

Takada, Y., A. Mukhopadhyay, G.C. Kundu, G.H. Mahabeleshwar, S. Singh, and B.B. Aggarwal. 2003. Hydrogen peroxide activates NF-kappa B through tyrosine phosphorylation of I kappa B alpha and serine phosphorylation of p65: evidence for the involvement of I kappa B alpha kinase and Syk protein-tyrosine kinase. *J. Biol. Chem.* 278:24233–24241. doi:10.1074/jbc.M212389200

Tassi, S., S. Carta, L. Delfino, R. Caorsi, A. Martini, M. Gattorno, and A. Rubartelli. 2010. Altered redox state of monocytes from cryopyrin-associated periodic syndromes causes accelerated IL-1beta secretion. *Proc. Natl. Acad. Sci. USA.* 107:9789–9794. doi:10.1073/pnas.1000779107

Thompson, R.J., J. Buttigieg, M. Zhang, and C.A. Nurse. 2007. A rotenone-sensitive site and H2O2 are key components of hypoxia-sensing in neonatal rat adrenomedullary chromaffin cells. *Neuroscience.* 145:130–141. doi:10.1016/j.neuroscience.2006.11.040

Todd, I., P.M. Radford, K.A. Draper-Morgan, R. McIntosh, S. Bainbridge, P. Dickinson, L. Jamhawi, M. Sansaridis, M.L. Huggins, P.J. Tighe, and R.J. Powell. 2004. Mutant forms of tumour necrosis factor receptor I that occur in TNF-receptor-associated periodic syndrome retain signalling functions but show abnormal behaviour. *Immunology.* 113:65–79. doi:10.1111/j.1365-2567.2004.01942.x

Touitou, I., S. Lesage, M. McDermott, L. Cuisset, H. Hoffman, C. Dode, N. Shoham, E. Aganna, J.P. Hugot, C. Wise, et al. 2004. Infevers: an evolving mutation database for auto-inflammatory syndromes. *Hum. Mutat.* 24:194–198. doi:10.1002/humu.20080

van de Loo, F.A., M.B. Bennink, O.J. Arntz, R.L. Smeets, E. Lubberts, L.A. Joosten, P.L. van Lent, C.J. Coenen-de Roo, S. Cuzzocrea, B.H. Segal, et al. 2003. Deficiency of NADPH oxidase components p47phox and gp91phox caused granulomatous synovitis and increased connective tissue destruction in experimental arthritis models. *Am. J. Pathol.* 163:1525–1537.

van de Veerdonk, F.L., S.P. Smeekens, L.A. Joosten, B.J. Kullberg, C.A. Dinarello, J.W. van der Meer, and M.G. Netea. 2010. Reactive oxygen species-independent activation of the IL-1beta inflammasome in cells from patients with chronic granulomatous disease. *Proc. Natl. Acad. Sci. USA.* 107:3030–3033. doi:10.1073/pnas.0914795107

Villalba, J.M., C. Parrado, M. Santos-Gonzalez, and F.J. Alcain. 2010. Therapeutic use of coenzyme Q10 and coenzyme Q10-related compounds and formulations. *Expert Opin. Investig. Drugs.* 19:535–554. doi:10.1517/13543781003727495

Yang, Q., Y.S. Kim, Y. Lin, J. Lewis, L. Neckers, and Z.G. Liu. 2006. Tumour necrosis factor receptor 1 mediates endoplasmic reticulum stress-induced activation of the MAP kinase JNK. *EMBO Rep.* 7:622–627.

Yazdanpanah, B., K. Wiegmann, V. Tchikov, O. Krut, C. Pongratz, M. Schramm, A. Kleinridders, T. Wunderlich, H. Kashkar, O. Utermöhlen, et al. 2009. Riboflavin kinase couples TNF receptor 1 to NADPH oxidase. *Nature.* 460:1159–1163. doi:10.1038/nature08206

Zhou, R., A. Tardivel, B. Thorens, I. Choi, and J. Tschopp. 2010a. Thioredoxin-interacting protein links oxidative stress to inflammasome activation. *Nat. Immunol.* 11:136–140. doi:10.1038/ni.1831

Zhou, R., A.S. Yazdi, P. Menu, and J. Tschopp. 2010b. A role for mitochondria in NLRP3 inflammasome activation. *Nature.* 469:221–225. doi:10.1038/nature09663